

Numerical analysis of concrete faced rockfill dams using gradient plasticity

Dakoulas, P., Stavrotheodorou, E. and Giannakopoulos, A.E.

Department of Civil Engineering, University of Thessaly, Volos 38334, Greece

E-mail: dakoulas@uth.gr

ABSTRACT: The behavior of concrete face rockfill dams is investigated numerically using Lade's constitutive model, which allows a realistic simulation of the stress-strain and volumetric-shear strain behaviour of rockfill in a wide range of confining stresses. The model is implemented in ABAQUS employing the Runge-Kutta-Dromand-Prince integration scheme. An enhancement based on gradient plasticity is proposed for preventing numerical difficulties on specific elements subjected to high shearing. The study examines the performance of two 200m-high CFRDs built in a narrow canyon, the first made of excellent quality rockfill and the second of average quality rockfill. The analysis simulates the staged construction, impoundment and anticipated creep and dynamic settlements. Similar analyses are repeated for dam heights of 100m and 300m, and the results are compared with field measurements. The study shows the effect of rockfill stiffness and dam height on the compressive stresses in the slab and relates the location of such high compression to the location of observed concrete slab failures in specific dams. It is concluded that the use of excellent quality rockfill at small void ratios (0.2) results to small construction settlements and relatively small deflections and compressive stresses in the slab even in the case of extra tall (300 m) dams.

Introduction

Designed to prevent water leakage into the interior of the dam, the concrete face slab is the most critical element in the performance and safety of concrete face rockfill dams (CFRDs). Naturally, its behavior depends significantly on the deformational response of the underlying gravel and rockfill materials. Recent incidents of crack development in the concrete face slab observed in high CFRDs, such as the 202m-high Campos Novos Dam (Brazil), the 186m-high Barra Grande Dam (Brazil) and the 145m-high Mohale Dam (Lesotho), are attributed to excessive deformation of the rockfill material. For example, Campos Novos Dam that was built from basalt rockfill having a low average modulus of 50-60 MPa [11], experienced failure of the central vertical joint due to compression along the vertical joints during impoundment, as shown in Fig. Due to compression in the longitudinal direction of the panels, several panels experienced shifting and superposition by 0.12 to 0.15 m at about 30% to 40% of the dam height over a length of 300 m (Fig. 1). As a result, there was rupture of the water stops and significant leakage of about 1500 lt/s. For dams in earthquake regions, seismic transient stresses and additional stresses due to accumulated dynamic settlements may increase further the compression along the walls of the vertical joints causing shear failure spalling [3,4], as in the case of the 156m-high Zipingpu Dam (China) during the May 12, 2008 Wenchuan earthquake [7,13].

Undoubtedly, proper modeling of the deformational characteristics of the underlying rockfill materials under generalized loading conditions is essential to successful face-slab performance predictions. During the past decades, the analysis of CFRDs has been based on simplified constitutive models for the rockfill material, such as the widely used hyperbolic Duncan and Chang model [5,6]. The main advantage of the latter model is the considerable accumulated experience regarding the required parameters for various types of rockfill materials, for which laboratory testing is difficult [6]. However, this is a simple model based on nonlinear elasticity, which is incapable of representing some important aspects of soil behavior such as the dilation and softening during shear.

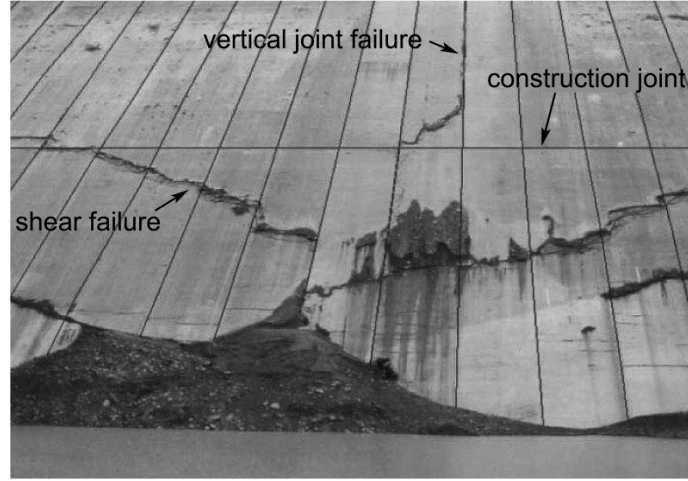


Figure 1: Concrete face slab failure due to compression at Campos Novos Dam

This study uses Lade's elasto-plastic model for the rockfill materials subjected to a wide range of confining stresses. In addition, it employs an optional gradient plasticity tool for improving numerical stability in regions of intense material softening behaviour.

Numerical model

Lade's model for rockfill

Lade's elasto-plastic isotropic hardening model with a single yield surface has been developed based on extensive sets of data from experiments on frictional materials including sand, clay, concrete and rock [8]. The model adopts a single yield surface, which is shaped as an asymmetric tear-drop, with the pointed axis at the axes origin in the stress space. The value of the plastic work derived from both shear and volumetric strains is the hardening parameter that is used to define the yield surface characteristics. The model adopts a non-associated flow rule based on a potential function that is shaped as a cigar with an asymmetric cross-section. Although the model is primarily aimed at frictional materials, a cohesion term may be easily accommodated by an appropriate shift of the axis of origin in the principal stress space. A detailed description of its incremental form is given by Lade and Jakobsen [8]. The 3D principal stress space formulation of Lade's model is implemented here as a user-defined material in the finite-element program ABAQUS [1]. Due to better accuracy and lower computational cost, the present study adopts the Runge-Kutta-Dormand-Prince scheme for Lade's constitutive model implementation in the three-dimensional principal stress space.

Gradient plasticity

Strain localization in granular materials is associated with plastic strain concentration in narrow shear bands and rupture. For the analysis of earth and rockfill dams, such plastic strain concentrations may develop near the abutments and along sharply inclined interfaces of material zones of different stiffness. Here, a simple gradient theory by Bassani [2] is adopted merely for the purpose of preventing numerical difficulties at critical locations. This methodology allows a local increase of hardening in finite elements experiencing very intense plastic strain gradient, as described below. Based on the gradient of the equivalent deviatoric plastic strain e_q^p within a finite element, a coefficient c_1 is computed from the expression

$$c_1 = \left[1 + l^2 \left(\frac{g_r}{\gamma_0} \right)^2 \right]^{1/2} \quad (1)$$

where l = intrinsic length scale, which may be the average or maximum particle diameter; γ_0 = reference strain, representing the range of the essentially elastic region of the material; and g_r = the norm of the gradient of e_q^p . The coefficient c_1 is used to modify the hardening behavior of the material in two different ways:

(a) The plastic modulus H is modified as follows

$$H^* = \begin{cases} Hc_1 & \text{for hardening} \\ H / c_1 & \text{for softening} \end{cases} \quad (2)$$

thereby increasing the hardening modulus or decreasing the softening modulus at elements with high values of g_r .

(b) In the case that some small artificial cohesion a is used for numerical stability, the effective cohesion is modified as $a^* = ac_1$. This artificial cohesion, which takes relatively small values (e.g. $a = 5$ kPa) compared to the rockfill shear strength, may be helpful for numerical stability during the simulation of the staged construction of the embankment slopes. Note that for uniform distribution of the equivalent deviatoric plastic strain, $c_1 = 1$. This simple gradient plasticity scheme has been proven to be effective in preventing numerical problems associated with local element straining associated with abrupt change in material stiffness near the abutments or interfaces.

Gravel behaviour

Two actual rockfill materials with quite different stiffness characteristics are considered:

(a) *Rockfill A*: an excellent quality rockfill based on data from the shell of Oroville Dam [10]. Its particles are well rounded to rounded, well graded, having very high strength and isotropic behavior. This material was selected due to its high strength and very low compressibility, resulting to the excellent observed performance of Oroville Dam.

(b) *Rockfill B*: a medium quality rockfill based on data from the shell of Pyramid Dam [10]. The rockfill particles are relatively angular, poorly graded, weak and anisotropic with respect to their strength. This material was selected to represent a rockfill of medium to relatively high compressibility.

The derivation of Lade's model parameters for each of the two materials was based on published results from isotropic compression and four triaxial compression tests at confining stresses equal to 207, 965, 2896 and 4413 kPa, on specimens with maximum particle diameter equal to 0.15m and specimen diameter equal to 0.914m. The derived Lade's model parameters are given in Tables 1 and 2 (corresponding to zone 3B) for each of the two rockfill materials, respectively. Due to lack of space, Fig. 2 presents representative comparison of the experimental data (circles) and model predictions (solid curves) on the stress-strain behavior and volumetric strains from triaxial compression tests of rockfill A at only two of the four confining stresses, namely at 207 kPa and 2896 kPa. Similarly, Fig. 3 plots the experimental data and the model predictions for rockfill B at 207 kPa and 2896 kPa. The results in Figs. 2 to 3 show that the model can capture in a realistic way the stress-strain behavior and the volumetric strain at various levels of confining stress for both rockfill materials.

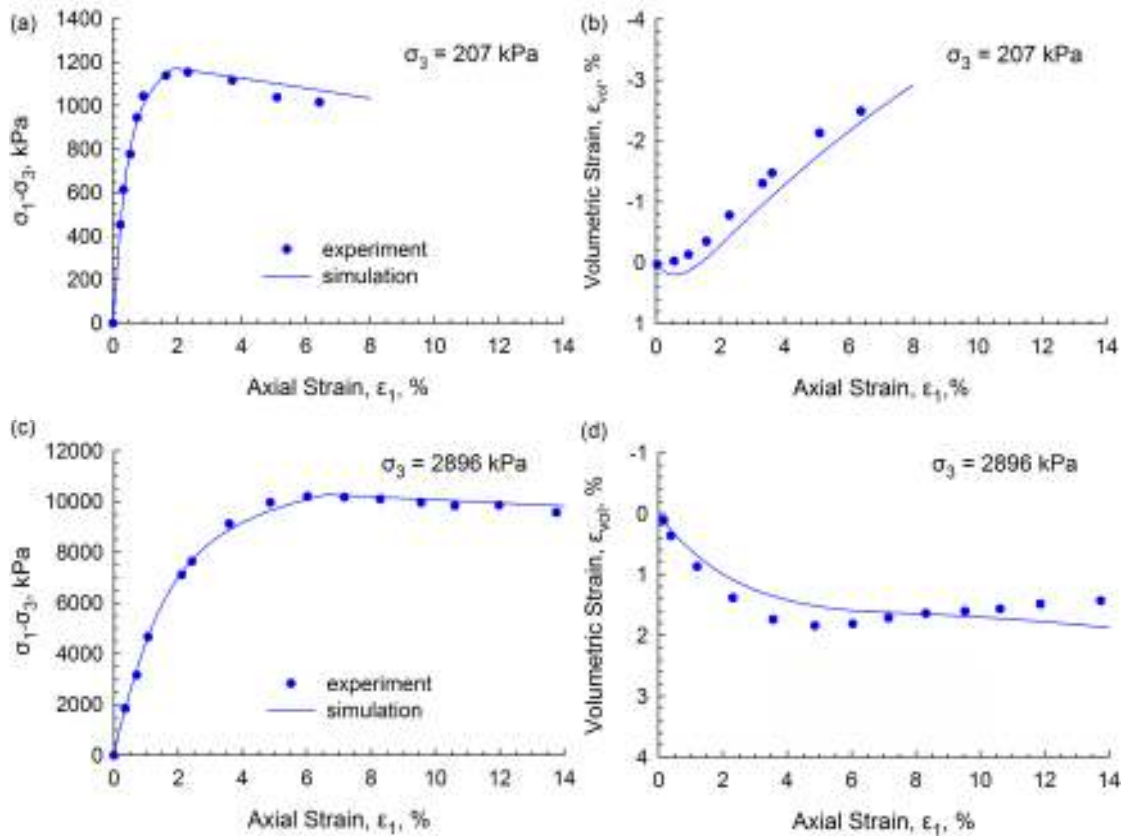


Figure 2: Rockfill A: Experiments and numerical predictions from triaxial compression tests at confining stress of 207 kPa and 2896 kPa

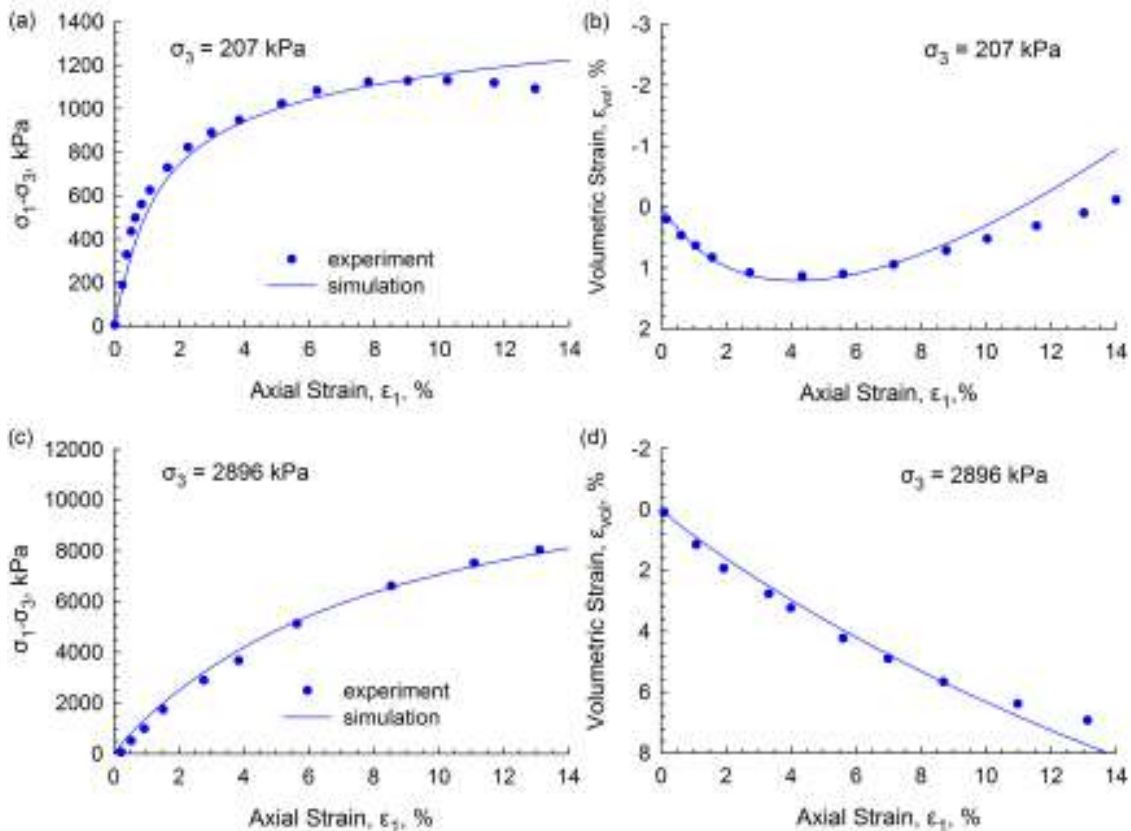


Figure 3: Rockfill B: Experiments and numerical predictions from triaxial compression tests at confining stress of 207 kPa and 2896 kPa

Concrete behaviour

The damage plasticity constitutive model for concrete by Lee et al. [9] is used for modelling the behaviour of the slab panels. The model takes into account the effects of strain softening, distinguishing between the damage variables for tension and compression. Moreover, it incorporates a degradation mechanism that represents the effects of damage on the elastic stiffness and its recovery of after crack closure. Fiber-reinforced concrete is used for the face slab by mixing plain concrete of compressive strength 37 MPa and fiber corresponding to a reinforcing index 2.5%. Based on Nataraja et al. [11], the fiber-reinforced concrete is estimated to have compressive strength of 42.4 MPa and tensile strength of 3.7 MPa.

Dam geometry

Fig. 4a illustrates the cross-section and the material zones of the dam, which has a height of 200 m and is built in a narrow canyon of trapezoidal shape with aspect ratio equal to $L/H=2$. The main material zones considered for the numerical analysis are the upstream rockfill zone 3B, the downstream rockfill zone 3C and the transition gravel zone 2B beneath the slab. The material properties for each zone are given in Tables 1 and 2, corresponding to the rockfill materials A and B, respectively. The upstream slab consists of 28 independent concrete panels. The slab panels have a width of 15 m and a variable thickness given by $t = 0.30 + 0.003h$, where h is the height of the overlying water. Fig. 4b illustrates the numerical discretization of the half of the dam geometry considering its symmetry with regard to mid-section.

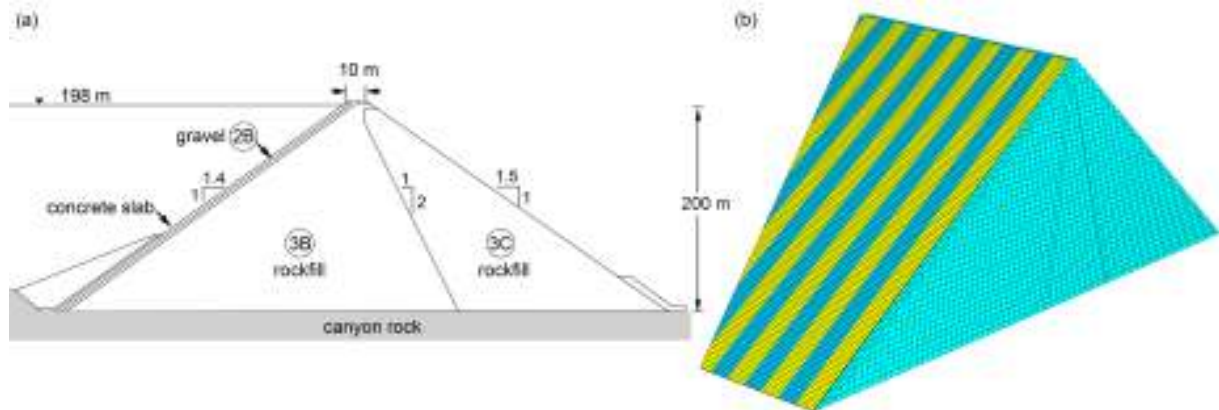


Figure 4: (a) Cross-section and material zones (b) Numerical model of the 200m-high dam

Table 1. Model parameters for dam built with rockfill type A

Zone	ρ Kg/ m^3	m	η_1	M	λ	ν	ψ_2	μ	C	p	b	h	α
3B	2435	0.3	167.3	1340	0.19	0.24	-3.06	2.7	$4.2 \cdot 10^{-5}$	1.7	0.2	0.85	0.6
2B	2435	0.3	167.3	2010	0.19	0.24	-3.06	2.7	$4.2 \cdot 10^{-5}$	1.7	0.2	0.85	0.6
3C	2435	0.3	167.3	1005	0.19	0.24	-3.06	2.7	$4.2 \cdot 10^{-5}$	1.7	0.2	0.85	0.6

Table 2. Model parameters for dam built with rockfill type B

Zone	ρ Kg/ m^3	m	η_1	M	λ	ν	ψ_2	μ	C	p	b	h	α
3B	2150	0.239	163.0	700	0.12	0.24	-3.06	3.0	$1.2 \cdot 10^{-4}$	1.8	0.1	0.70	0.8
2B	2150	0.239	163.0	1050	0.12	0.24	-3.06	3.0	$1.2 \cdot 10^{-4}$	1.8	0.1	0.70	0.8
3C	2150	0.239	163.0	525	0.12	0.24	-3.06	3.0	$1.2 \cdot 10^{-4}$	1.8	0.1	0.70	0.8

Analysis and results

Figs. 5a and 5b plot the distribution of settlements at the end of construction for the two dams made of rockfill A and B, with maximum settlements equal to 0.60m and 1.99m, respectively. The behavior of the dam made of rockfill A (Oroville material) appears to be excellent, with a maximum settlement to height ratio $S_c/H=0.30\%$. This is comparable to the settlement ratio of the actual 244m-high (earth-core rockfill) Oroville dam (California) that was $S_c/H=0.31\%$. On the other hand, the behavior of the Pyramid rockfill dam is rather average with a settlement to height ratio $S_c/H \approx 1\%$. Fig. 6 shows the effect of dam height and rockfill stiffness on the maximum construction settlement, based on the numerical predictions of three dams having heights equal to 100m, 200m and 300m, considering both rockfill A (blue circles) and rockfill B (blue triangles). The shaded area represents the range of variation between the two different qualities of rockfill. Also shown in Fig. 6 are available measurements of construction settlements from existing CFRDs with void ratios e between 0.18-0.25 (circles) and between 0.25-0.31 (triangles). Moreover, the construction settlements of Campos Novos, Barra Grande and Mohale dams, which experienced failure in the concrete slab during first impoundment, are shown in the figure. All reported measurements in Fig. 6 correspond only to dams in narrow canyons with a shape factor $0.9 < A_s/H^2 < 4$.

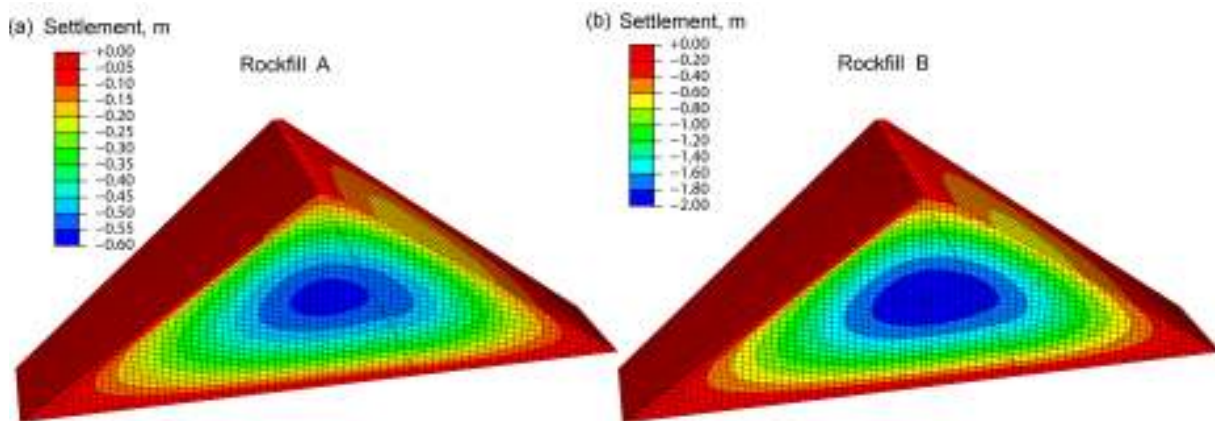


Figure 5: Construction settlements for the dam made of (a) rockfill A and (b) rockfill B.

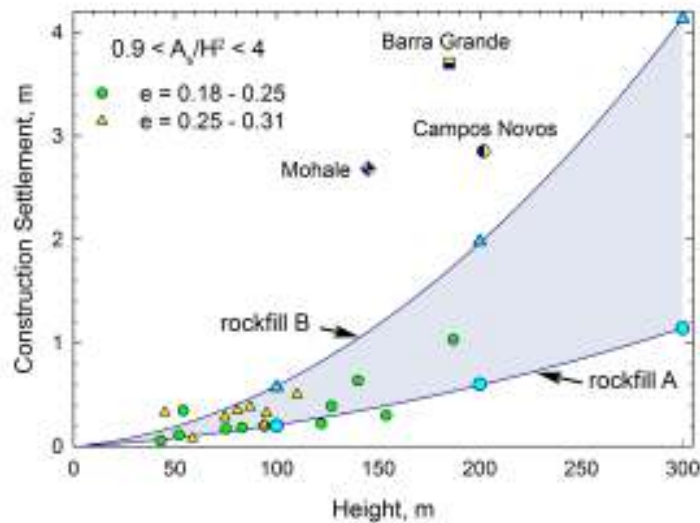


Figure 6: Computed and measured construction settlements of rockfill compacted at different void ratios versus dam height (for dams in narrow canyons).

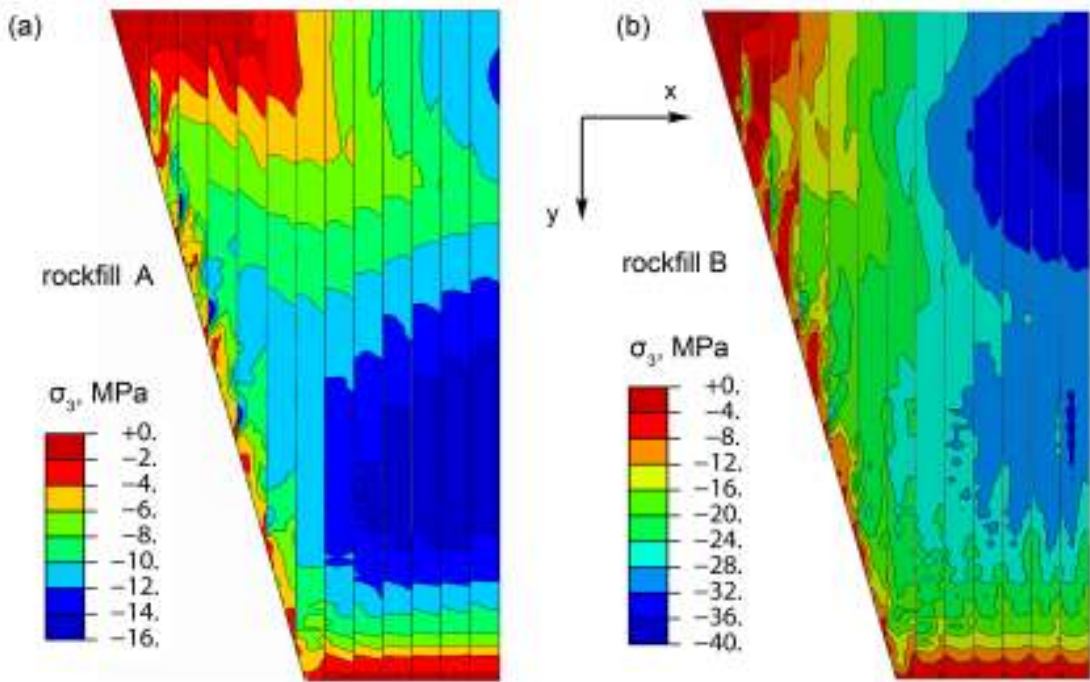


Figure 7: (a) Cross-section and material zones (b) Numerical model of the 200m-high dam

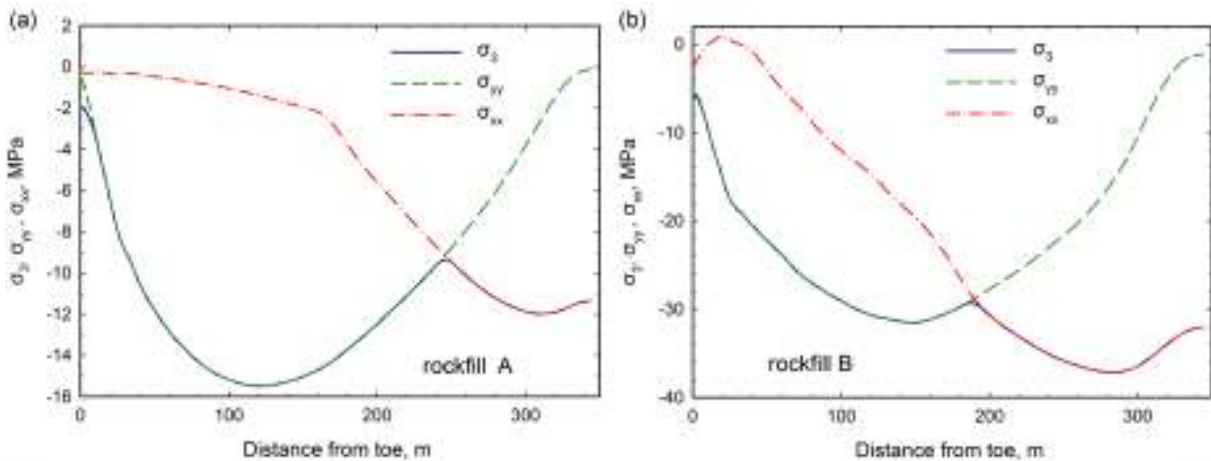


Figure 8: (a) Cross-section and material zones (b) Numerical model of the 200m-high dam

It is evident from Fig. 6 that dams compacted to lower void ratios tend to yield settlements that are closer to the results of rockfill A, whereas dams compacted to higher void ratios yield settlements that are closer to those of rockfill B. It is also shown that the construction settlements of Campos Novos, Barra Grande and Mohale dams are much higher than the range of the measured and numerically predicted settlements.

The maximum post-impoundment settlement, consisting of creep and possible dynamic settlements, is assumed here to be equal to 50% of the maximum construction settlement. Fig. 7 plots the distribution of maximum compressive stresses in the slab due to post-impoundment settlements. Moreover, Fig. 8 plots the distribution of the minor principal stress σ_3 , and stresses σ_{yy} and σ_{xx} (see directions x,y in Fig. 7) along the length of concrete panel at mid-section. The results show the maximum compression due to impoundment occurs due to stresses σ_{yy} in the longitudinal panel direction, at about 40% of the dam height. By

contrast, the maximum compression due to post-impoundment settlement is caused by increase in σ_{xx} at the upper part of the slab. Based on results from all analyses, for extra tall dams this increase of σ_{xx} is more critical than the maximum compression given by σ_{yy} .

Conclusions

1. The use of Lade's constitutive model for modelling the behaviour of rockfill allows a very realistic simulation of the experimental results in terms of the stress-strain behavior and volumetric strains in a very wide range of confining stresses.
2. The use of excellent quality rockfill at small void ratios (0.2) results to small construction settlements and relatively small deflections and compressive stresses in the slab even in the case of extra tall (300 m) dams.
3. The design of CFRDs of average-quality, compressible rockfill at heights equal or larger than 200m is not recommended, unless special provisions are undertaken.

Acknowledgements

This research has been co-financed by the European Union (European Social Fund – ESF) and Greek national funds through the Operational Program "Education and Lifelong Learning" of the National Strategic Reference Framework (NSRF)-Research Funding Program: Heracleitus II. Investing in knowledge society through the European Social Fund.



References

- [1] ABAQUS (2014). Users' Manual, Simulia, Providence, RI, USA.
- [2] Bassani JL. (2001). Incompatibility and a simple gradient theory of plasticity, Journal of Mechanics and Physics of Solids, 49:1983-1996.
- [3] Dakoulas P. (2012) Nonlinear seismic response of tall concrete faced rockfill dams in narrow canyons, Soil Dynamics and Earthquake Engineering, 34:11-24.
- [4] Dakoulas P. (2012). Longitudinal vibrations of tall concrete faced rockfill dams in narrow canyons, Soil Dynamics and Earthquake Engineering, 41:44-58.
- [5] Duncan JM, Chang CY. (1970). Nonlinear analysis of stress and strain in soils, J. of Soil Mech. and Found. Engineering, ASCE; 96(5):1629-1653.
- [6] Duncan JM, Byrne P, Wong K, Mabry P. (1980). Strength, stress-strain and bulk modulus parameters for finite element analyses of stresses and movements in soil masses, Report UCB/GT/80-01, Univ. of California, Berkeley, Ca, USA.
- [7] Guan Z. (2009). Investigation of the 5.12 Wenchuan Earthquake damages to Zipingpu Water Control Project and an assessment of its safety state, Science in China, Series E, Technological Sciences, 52(4):820-834.
- [8] Lade PV, Jakobsen KP. (2002). Incrementalization of a single hardening constitutive model for frictional materials, Num. and Anal. Methods in Geomechanics, 26:549-659.

- [9] Lee J, Fenves GL. (1998). A plastic-damage concrete model for earthquake analysis of dams, *Journal of Earthq. Eng. & Struct. Dynamics*, 27: 937-596.
- [10] Marachi ND, Chan CK, Seed HB. (1972). Evaluation of Properties of Rockfill Materials, *J. of Soil Mech. and Found. Div., ASCE*, 98:95-114.
- [11] Nataraja MC, Dhang N, Gupta AP. (1999). Stress-strain curves for steel-fiber reinforced concrete under compression, *Cement & Concrete Composites*, 21:383-390.
- [12] Sobrinho JA, Xavier LV, Albertoni C, Correa C, Fernandes R. (2007). Performance and concrete repair at Campos Novos, *Hydropower Dams*, 2.
- [13] Wieland, M. (2009). Concrete faced rockfill dams in highly seismic regions, 1st Intern. Symposium on Rockfill Dams, Chengdu, China, October 18-21.